EXTENSION OF THE OPERATING SPACE OF HIGH-BETAN FULLY NON-INDUCTIVE SCENARIOS ON TCV USING NEUTRAL BEAM INJECTION

C. PIRON
Consorzio RFX
Padova, Italy
Email: chiara.piron@igi.cnr.it

J. GARCIA
CEA-IRFM
Saint-Paul-lez-Durance, France

T. GOODMAN
EPFL-SPC
Lausanne, Switzerland

M. AGOSTINI, M. GOBBIN, L. PIGATTO, M. VALLAR
Consorzio RFX
Padova, Italy

G. GIRUZZI, J. MORALES
CEA-IRFM
Saint-Paul-lez-Durance, France

M. FONTANA, A. KARPUSHOV, M. KONG, M. MERLE, O. SAUTER, D. TESTA
EPFL-SPC
Lausanne, Switzerland

S. NOWAK
IFP-CNR
Milano, Italy

M. YOSHIDA
QST
Naka, Japan

THE TCV TEAM

THE EUROFUSION MST1 TEAM
See the author list "H. Meyer et al 2017 Nucl. Fusion 57 102014"

Abstract

The fully non-inductive sustainment of high normalized beta plasmas (betaN) is a crucial challenge for the steady-state operation of a tokamak reactor. In order to assess the difficulties found on such scenarios, steady-state regimes have been explored at the Tokamak à Configuration Variable (TCV) using the newly available 1MW Neutral Beam Injection (NBI) system. The operating space is extended towards plasmas that are closer to those expected in JT-60SA and ITER, i.e. with significant NBI and Electron Cyclotron Resonance Heating and Current Drive (ECRH/CD), bootstrap current and Fast Ion (FI) fraction. BetaN values up to 1.4 and 1.7 are obtained in lower single null L-mode ($H_{98}(y,2)$~0.8) and H-mode ($H_{98}(y,2)$~1) plasmas, respectively, at zero time averaged loop voltage and q_{95}~6. Fully non-inductive operation is not achieved with NBI alone, whose injection can even increase the loop voltage in presence of EC waves. A strong contribution to the total plasma pressure of bulk and FIs from NBI is experimentally evidenced and confirmed by interpretative ASTRA and NUBEAM modelling, which further predicts that FI charge-exchange reactions are the main loss channel for NBH/CD efficiency. Internal transport barriers, which are expected to maximize the bootstrap current fraction, are not formed in either the electron or the ion channel in the plasmas explored to date, despite a significant increase in the toroidal rotation and FIs fraction with NBI, which are known to reduce turbulence. First results on scenario development of high-betaN fully non-inductive H-mode plasmas are also presented.

1. INTRODUCTION

The fully non-inductive sustainment of high normalized beta (betaN) plasmas is a crucial challenge for the steady-state operation of a tokamak reactor. In this scenario the plasma current is sustained without any external poloidal magnetic flux consumption for several characteristic plasma current diffusion times. To achieve a time-averaged zero loop voltage (V_{loop}), the maximization of poloidal beta (betap) is also suitable in order to maximize the fraction of bootstrap current and alleviate the necessity of external current drive. However, such a process is notoriously complicated due to the exigent physics requirements: high input power and plasma confinement, current alignment between bootstrap current and current drive and MHD control. In order to assess the difficulties found on such scenarios and to extend previous steady-state plasmas obtained with only Electron Cyclotron Resonance Heating (ECRH), steady-state regimes have been explored at the Tokamak à Configuration Variable (TCV) using the newly available Neutral Beam Injection (NBI) system [1, 2]. This system supplies up to 1MW (25keV) to the plasma by accelerating positive deuterium ions. Due to machine protection constraints [2], the maximum NB injected energy was initially limited to 0.5MJ and then to 0.8MJ in the experiments presented in this work. Being the beam duct port installed at the torus middle plane, off-axis NBI is obtained on TCV by vertically shifting the plasma magnetic axis (z), values up to |z|=13cm have been explored. In this work, fully non-inductive operation is achieved with additional 3.2 MW of ECRH power [3], which is transferred to the plasma through both X2 (P=2.3 MW) and X3 (P=0.9 MW) waves. It is worth noticing that X3 waves do not provide any net current drive on TCV, being their wave vector aiming at the plasma core perpendicularly to the magnetic field to maximize the power absorption. The EC wave cut-off from the plasma is n_e>4.3e19m^{-3} and n_e>1.1e20m^{-3} for the X2 and X3 mode, respectively. This paper presents the first results that have been achieved during the dedicated experiments of the 2017/18 EUROfusion MST1 campaign on TCV and it is organized as it follows: Section 2 describes the explored plasma scenarios and it presents the resulting extended operating space. The role of the NBI to both plasma current drive and pressure is investigated and documented with both data analyses and modeling in Section 3. The challenge of generating Internal and External Transport Barriers (I/ETBs), which are crucial to improve the plasma confinement and the total fraction of non-inductive current drive, is discussed in Section 4. The summary and outlook are finally given in Section 5.

2. THE EXTENDED OPERATING SPACE

Compared to the past, when fully non-inductive plasmas were sustained using EC waves only on TCV [4, 5], the operating space has been now extended towards higher plasma current (Ip = [130, 150] kA) and density ($n_{e,0}$ ~ [2, 3]e19 m^{-3}) using co-Ip NBI; this produces plasmas closer to those expected in JT-60SA and in ITER, i.e. with significant NBI and ECRH current drive, bootstrap current and fast ion fraction. This new plasma scenario is designed to minimize the first-orbit and shine-through beam losses. Furthermore, lower single-null plasmas at B_0=1.4T were chosen over the previously studied limiter ones, since the lower neutral penetration from the edge is expected to reduce the Charge eXchange (CX) beam losses [6]. Both L-mode and H-mode plasmas have been explored. A representative Ip=130kA L-mode discharge is shown in Fig.1 a-c), which reports the time evolution of a) the plasma current and the bootstrap current fraction (f_{BS}) (left y-axis, black and cyan) and the on-axis electron density from the Thomson Scattering diagnostic (right y-axis, blue).

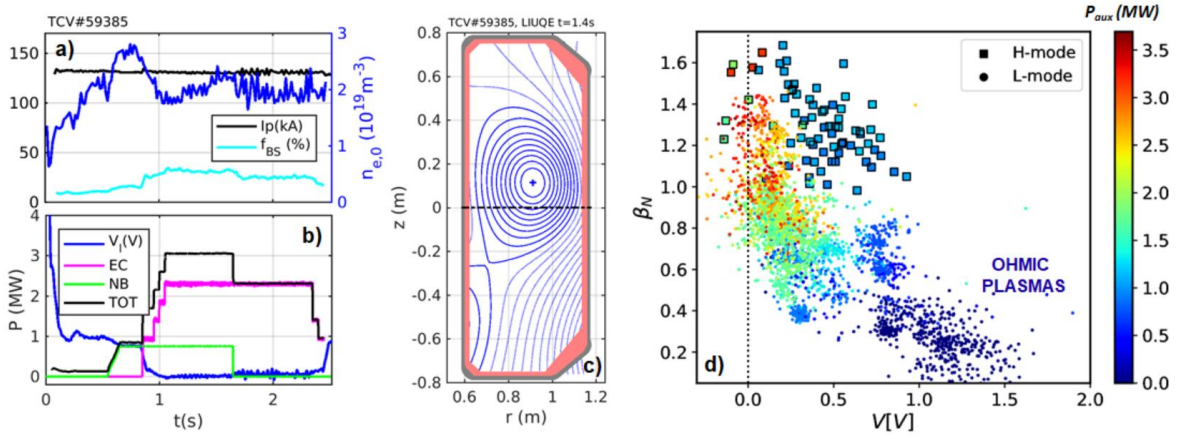

FIG. 1. Time evolution of a) plasma current and the bootstrap current fraction (black and cyan, left y-axis), on-axis electron density from the Thomson Scattering diagnostic (blue, right y-axis); b) loop voltage (blue), electron cyclotron power (magenta), neutral beam power (green) and total power (black); d) LIUQE equilibrium at t = 1.4 s, poloidal view of the NBI

injection line (dashed black line); d) Time averaged normalized beta as a function of loop voltage in the explored L-mode (points) and H-mode (squares) plasmas. The colour code corresponds to the total injected power $P_{aux} = P_{NB} + P_{EC}$

As it can be inferred from the time evolution of the loop voltage (blue) and the auxiliary powers (EC in magenta, NB in green and the total in black), which are shown in Fig.1 b), stationary non-inductive operation is achieved for around 10 current diffusion times (around 150 ms on TCV heated plasmas), by combining 2.3 MW of on-axis EC power (0.9 MW from EC-X3 waves) with 0.8 MW of off-axis NB power, both injected in the co-Ip direction. The off-axis NB injection line projected in the poloidal plane (black dashed line) is reported together with the lower single null equilibrium reconstructed by LIUQE [7] at t = 1.4 s in Fig. 1 c). Bootstrap current fraction is around f_{BS}=40% in this discharge.

The plasma performance of the plasmas explored in this work is summarized in Fig. 1 d), which shows betaN as a function of V_{loop}, both averaged over 15 ms around each acquisition time of the Thomson Scattering diagnostic. The exploration of the operating space has been carried out by carefully scanning $P_{aux} = P_{EC} + P_{NB}$, the NB power fraction (P_{NB} / P_{aux}) and the radial deposition locations of the NB and EC Heating and Current Drive (H/CD). BetaN values up to 1.4 and 1.7 have been reached in fully non-inductive plasmas ($V_{loop} \sim 0$) in L-mode and H-mode respectively, both at $q_{95} \sim 6$, f_{BS}<40-50%, in presence of good confinement ($H_{98}(y,2) \sim 0.8$ in L-mode and $H_{98}(y,2) \sim 1$) using central EC and NB H/CD in the co-Ip direction. For comparison, it is worth noticing that betaN < 0.4 and $V_{loop} > 0.7$V are typically obtained in similar Ohmic plasmas (blue points).

3. THE ROLE OF THE NEUTRAL BEAM INJECTION TO THE SCENARIO DEVELOPMENT

3.1. NBI contribution to the non-inductive current drive

Developing steady-state scenario at high betaN is a complexity task. Indeed adding NBI results to an increase or decrease of V_{loop} depending on other plasma parameters, like the plasma vertical position (z), the electron temperature (T_e), density and the presence of ECH/CD. Fully non-inductive operation could not be achieved with NBI alone ($V_{loop} > 0.5$ V). Data analyses of the explored plasmas show that when adding NBI to the Ohmic phase the lower the density, the faster the V_{loop} drop during the NBI. Nonetheless, it is worth noticing that the former can not be arbitrarily decreased, being limited by the maximum shine-through power loss limit (P_{ST} < 10%). Fig. 2 a) shows the averaged absolute loop voltage variation obtained during NBI with (magenta triangles and diamonds) and without (green squares) ECRH as a function of a diagnostic proportional estimate of the Spitzer's NB slowing time [8] in the plasma core, which is quantified here like $T_{e,0}^{3/2} n_{e,0}^{-1}$. Notice that is quantity is rescaled of a factor of 10 in presence of EC waves to compensate for the relatively higher $T_{e,0}$. The figure suggests that an optimal balance between the non-inductive current drive and the NB slowing time can be found using NBI only, which decreases ΔV_{loop} up to 0.3 V. Conversely, any clear dependence of the loop voltage variation on the NB slowing time is not observed in presence of EC waves. Interestingly, the loop voltage increases with on-axis NBI (|z| < 3 cm, magenta triangles) while it decreases with off-axis injection (magenta diamonds), yet only up to -0.1 V. These pieces of evidence were investigated with ASTRA interpretative modelling [9] of equilibrium, bulk ion temperature and FIs. The results for a representative discharge are reported in Fig. 2 on the right. Panel b) of this figure shows the time evolution of the EC (magenta) and NB (green) power, together with the measured (blue) and the modelled (cyan) loop voltage, which clearly increases after t = 1.2 s. The electron temperature and density profiles from the Thomson Scattering diagnostic before (t = 1 s, solid line) and after (t = 1.5 s, dashed line) the NBI, which are reported in panels c-d), shows that the core plasma density is pumped-out during ECRH [10] (see also Fig. 1 a)), while it is fuelled during NBI (up to 30% at constant gas injection). As it shown in panel d), which reports the EC current density profiles (magenta) from the linear TORAY-GA ray tracing code [11], this mechanism (solid line) helps achieve high electron temperature plasmas (solid line in panel c)) and thereby high core ECCD efficiency ($j_{ECCD} \sim T_e/n_e$), wheras on-axis NBI fuelling (dashed line) counteracts it, ultimately reducing the ECCD efficiency. Since the NBCD (green dashed line) is insufficient to compensate for the decreased ECCD, the loop voltage increases. The same panel reports also the evolution of the q-profile (solid and dashed blue lines), which hinders any further boostrap current increase by relaxing from weakly reversed to fully monotonic. This evidence might explain why internal transport barriers, for which the q-profile reversal is crucial, were not observed in the plasmas explored up to date, being an excessive on-axis NBCD detrimental for their onset, as previously shown in modelling [12]. The counteracting interplay between the ECCD efficiency and the NBI fuelling is relatively weaker with off-axis injection, which therefore results to slightly negative ΔV_{loop} values (empty magenta diamonds).

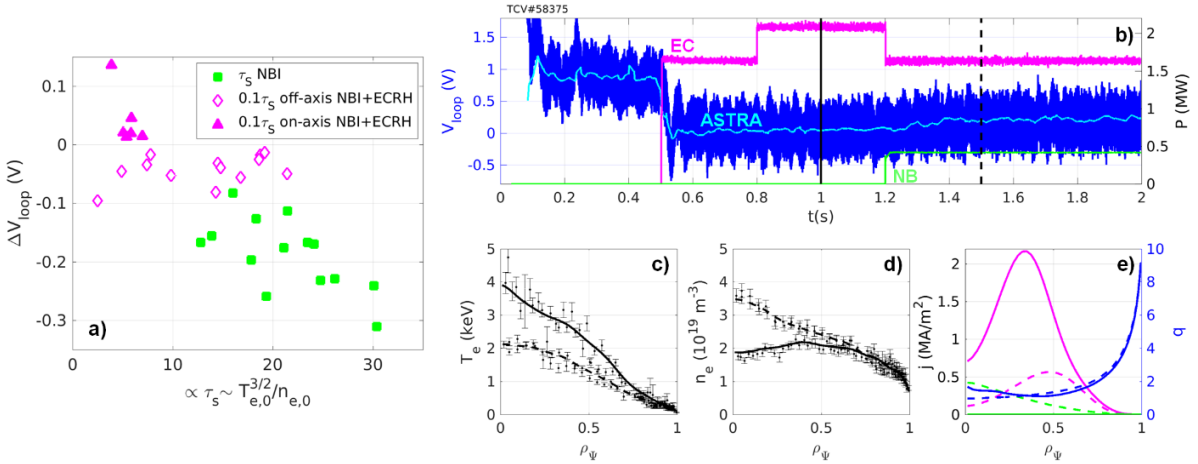

FIG. 2 Left: a) absolute loop voltage change during NBI as a function of a proportional estimate of the NB slowing time on TCV Ohmic (green squares) and ECRH heated plasmas (magenta triangles)). Right: b) time evolution of the loop voltage (left y-axis, measured in blue, modeled by ASTRA in cyan), ECRH and NBI power (right y-axis, in magenta and green), plasma profiles before (t=1s solid line) and after (t=1.5s dashed line) NBI, c-d) electron temperature and density profiles from Thomson Scattering diagnostic, e) ASTRA modeling of the EC and NB current density profiles (left y-axis, magenta and green) and q- profile (right y-axis, blue).

3.2. NBI contribution to the total plasma pressure

Statistical analyses of experimental data show that the highest betaN does not necessarily correspond to having the maximum electron thermal energy. This suggests a strong contribution of bulk and FIs to the total plasma pressure. This experimental evidence is confirmed by ASTRA interpretative modelling. Simulations, like the one shown in Fig.2 a), predict a large population of FIs (light-blue) with a density comparable to the bulk (green). This result is also confirmed by NUBEAM used as a stand-alone Monte Carlo FI simulator [13, 14]. Modelling further reveals that FI CX reactions are the main loss channel reducing NB heating efficiency, as it can be seen in Fig. 2 b) which shows the time evolution of the different NB power redistribution channels (CX losses in yellow, sum of ion first orbit and shine-though losses in blue, NB power absorbed by ions and electrons in green and red). Interestingly, a large FI contribution and significant CX losses were also observed in inductive L-mode plasmas in a circular limited configuration at TCV [15]. Nonetheless, a quantitative comparison of the NBI performance on limiter and lower single null plasma equilibria is not straightforward due to the significantly different plasma parameters that were explored in the corresponding scenarios.

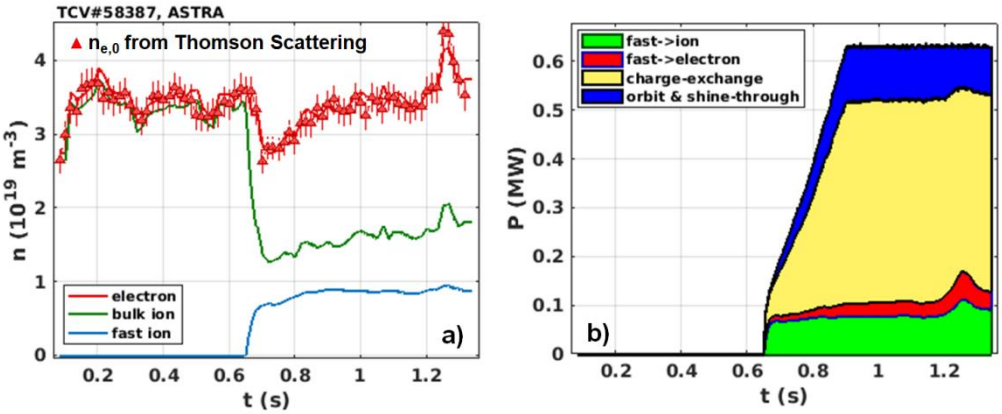

FIG. 3. Interpretative ASTRA simulation of a TCV L-mode discharge. Time evolution of a) core electron (red), bulk (green) and fast (blue) ion density. Experimental electron density measurements from the Thomson Scattering diagnostic (red triangles), b) NBI power redistribution channels: power to ions (green) and electrons (red), charge-exchange (yellow), first ion orbit and shine-through (blue) losses.

4. ON THE CREATION OF TRANSPORT BARRIERS

Thanks to their inherently steep gradients, plasmas with transport barriers are characterized by improved confinement and a large fraction of self-driven bootstrap current, which make the plasma compatible with continuous operation. When Internal or/and External Transport Barriers (I/ETBs) originate in a plasma, turbulent

transport is generally reduced in the plasma core or/and at the edge, respectively. An optimized shaping of current density and pressure profiles and a good alignment of the large fraction of bootstrap current with their gradients are crucial for achieving significant improvements in particle and energy confinement, as well as in self-current drive. In this work high-beta fully non-inductive scenarios with either ITB or ETB have been explored using both ECRH and NBI H/CD. The results are presented and discussed in the following sections.

4.1. Internal Transport Barriers (L-mode)

The creation of ITBs turned out to be a challenge as they were not formed in either the electron or the ion channel in the plasmas explored to date; and this in spite of a significant increase in the toroidal rotation and fast ion (FI) fraction with NBI, which are known to reduce turbulence [16]. The increase of the former is documented in Fig. 4, which reports the core toroidal plasma rotation measurements from the Charge eXchange Recombination Spectroscopy (CXRS) as a function of the total power $P_{TOT} = P_{OH} + P_{EC} + P_{NB}$. The colour code highlights the NB power fraction. Toroidal rotation velocity values of around +20km/s, i.e. in the counter-Ip direction, are obtained during the Ohmic phase of the plasmas explored in this work. The toroidal rotation reverts its direction in presence of co-Ip ECRH (blue points) or/and NBI, but interestingly the maximum values are obtained with NBI only (in brown), which accelerates the plasma core up to -200 km/s with 1MW on-axis injection. To investigate the possibility that the plasmas explored in this work are still Trapped Electron Mode (TEM) turbulence dominated, hence less prone to both NB torque and FI stabilization, transport and turbulence analyses have been started. Some of the most representative plasmas with different ECRH/CD and NBI configurations have been selected for such analysis. From the turbulence point of view, the plasmas shown in this paper are interesting as they combined mostly electron heating with a significant toroidal rotation and fast ion fraction, which have been shown to reduce turbulence that is driven only by the Ion Temperature Gradient (ITG) modes [16]. Therefore, the analyses of the impact of such turbulence suppression mechanisms can be extended to other plasma regimes. For that purpose, the CRONOS suite of codes [17] is applied here in order to perform transport analyses and as a tool for the preparation of the inputs required for extended gyrokinetic simulations. As a first step, CRONOS predictive simulations of current and electron and ion temperatures have been performed. Transport is modelled using the Current Diffusion Ballooning Mode (CDBM) model [18], which is known to well capture the transition to ITB regimes but also gives reasonable results for regular L-mode plasmas. ECRH/CD source is calculated with the TORAY-GA code, whereas NUBEAM is used to model NBI. The results of the CRONOS predictive simulation for the discharge that is reported in Fig. 3 are compared with interpretative ASTRA modeling and with diagnostic data in Fig. 5. This figure shows the time evolution of the loop voltage (measured in blue, ASTRA in yellow and CRONOS in red) in panel a), the electron (red) and ion (green) temperature profiles (CRONOS in solid line, Thomson Scattering diagnostic data with triangles down, CXRS ones with triangles down) in panel b) and the q-profile (CRONOS in blue, ASTRA in red and LIUQE in green) in panel c).

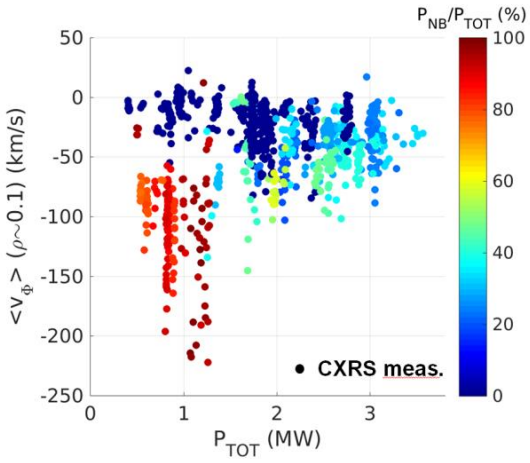

FIG. 4 TCV core plasma toroidal rotation from CXRS as a function of the total power PTOT = POH + PEC + PNB. The colour code corresponds to the NB power fraction.

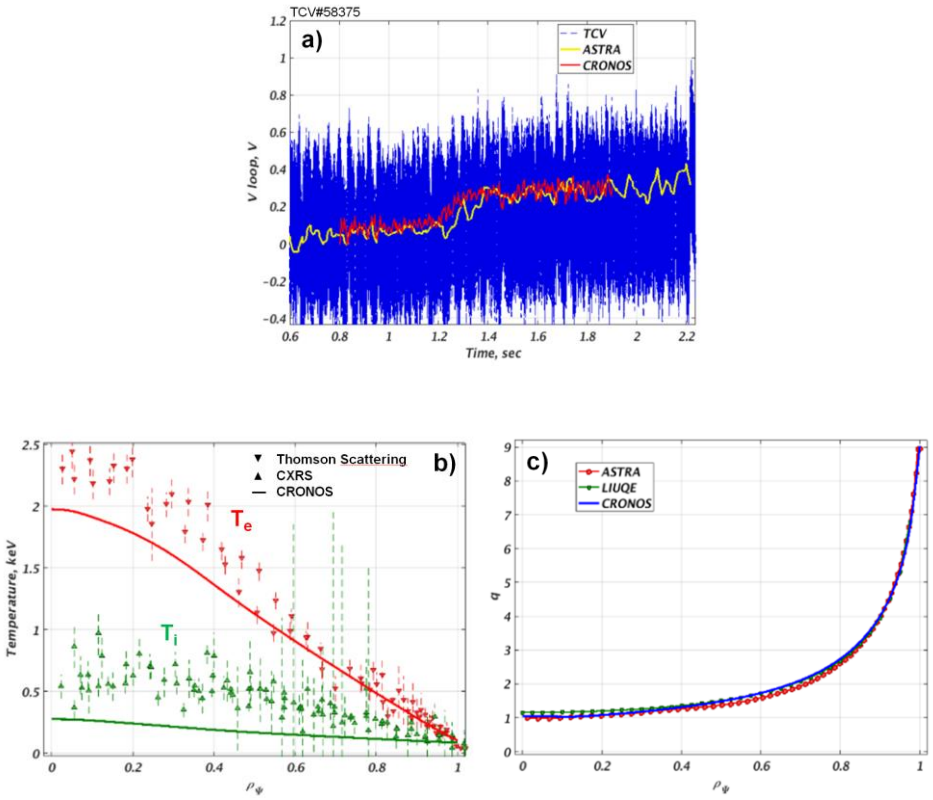

FIG. 5 a) The time evoution of the loop voltage, comparison between diagnostic data (blue), ASTRA interpretative modeling (yellow) and CRONOS predictive modeling (red). b) Electron (red) and ion (green) temperature profiles predicted by CRONOS (solid line) compared to the Thomson Scattering (triangles down) and CXRS (triangles up) data. c) Comparison between the q-profile obtained with LIUQE (green), ASTRA (red) and CRONOS (blue).

4.2. External Transport Barriers (H-mode)

Thanks to the newly available NBI system, the operating space of high-beta fully non-inductive scenarios could be extended for the first time on TCV towards H-mode plasmas. This scenario aims at betaN values higher than 2.5, i.e. at plasma pressure values closer to those expected in ITER during steady state operation at fusion gain Q>5 [19]. Due to the challenging onset of ITBs, the envisaged H-mode target scenario on TCV are plasmas with ETBs only at low central magnetic shear and $1 < q_0 < 2$. A challenging, yet possible, strategy to reproduce such scenario is to develop plasmas whose density remains lower than the X2 wave cut-off from the plasma even after the L/H-mode transition, so that ECCD can still contribute to the total non-inductive current drive fraction. One of the first attempts at this strategy is shown in Fig. 6. In this lower single null discharge at $q_{95} = 6$, relatively high pressure (betaN = 1.7) and good confinement ($H_{98}(y,2) = 1$) (magenta and green in panel d)) are sustained for several current diffusion times at nearly zero time averaged V_{loop} (green in panel a)) using nearly central co-Ip ECRH (P = 0.9 MW, magenta) and NBI (P = 1.2 MW, green). The time evolution of the auxiliary power is reported in panel b). The L/H-mode transition occurs a half current diffusion time after the NB injection. At that time type-I Edge Localized Modes (ELMs) appear, whose frequency is increased by the additional heating power from X3-waves (P = 0.45 MW), which is switched on slightly afterwards. As it is shown in panel c), the electron density (black) at the pedestal almost doubles during H-mode, while the temperature increases (green) by nearly 50%. Conversely, the increase in the core is comparable, as it can be inferred from panels e-f), which reports the electron temperature and density profiles during L- (blue) and H-mode (red). It is worth noticing that density remains below the EC-X2 wave cut-off from the plasma (black dashed line in panel f)) even during H-mode. ASTRA interpretative modelling of the EC (magenta), NBI (green) and bootstrap (cyan) current density profiles during H-mode is reported in Fig. 6 g) (left y-axis), together with the resulting q-profile (right y-axis, black). The latter is very slightly reversed in the core and close to 1 up to the normalized poloidal radius of around 0.5, therefore further scenario development is needed to meet the target, i.e. a more highly elevated q-profile with a lower central magnetic shear. The stationarity of this H-mode plasma is limited in this discharge by the MHD activity, indeed a 6 kHz n=1 neoclassical tearing mode,

which is likely triggered by the central EC power deposition, eventually locks to the wall ending the plasma discharge.

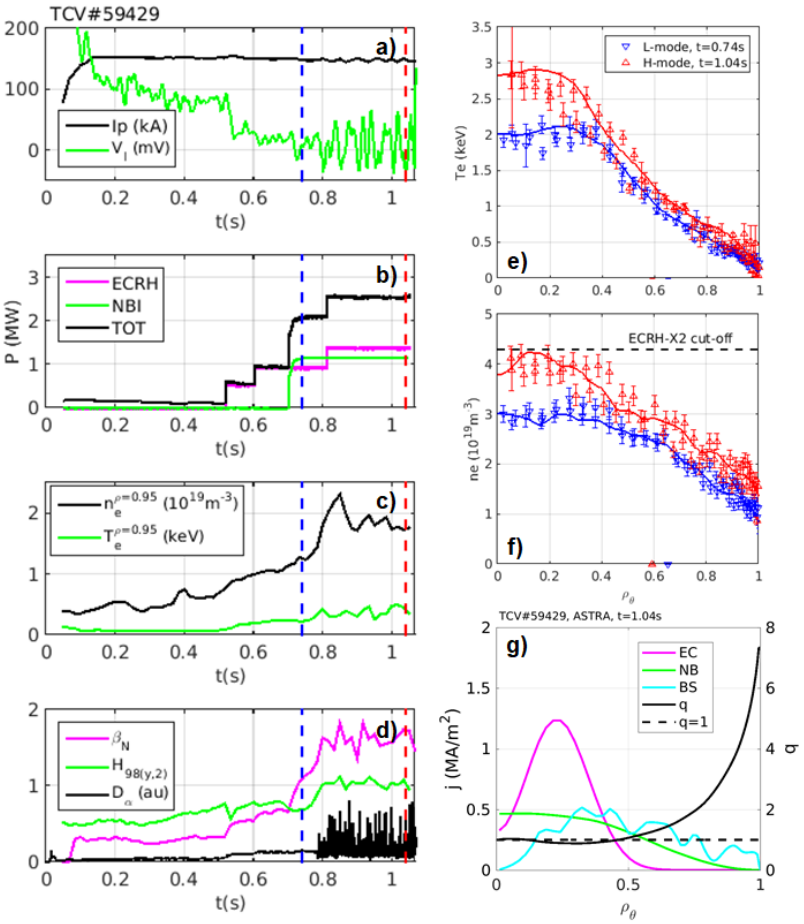

FIG. 6 TCV nearly fully non-inductive H-mode plasma. Time evolution of a) plasma current (black) and loop voltage (green); b) ECRH (magenta), NBI (green) and the total auxiliry (black) power; c) electron density (black) and temperature (green) at the pedestal; d) betaN (magenta), $H_{98(y,2)}$ (green) and D_α (black); e-f) electron temperature and density from the Thomson Scattering diasnostic during L-mode (t= 0.74 s, blue) and H-mode (t = 1.04 s red) the X2 wave cut-off from the plasma is also shown (black dashed line); g) ASTRA interpretative modeling of the current density (left y-axis: ECCD in magenta, NBCD in green, bootstrap in cyan) and the q profile (right y-axis in black) during H-mode, q=1 surface is also shown (dashed black line).

5. CONCLUSIONS

The operating space of high betaN fully non-inductive scenarios has been extended on TCV using the newly available 1MW NBI system. Plasma regimes closer to those expected in JT-60SA and ITER have been explored, i.e. with significant NBI and ECRH current drive, bootstrap current and fast ion fraction. BetaN values up to 1.4 and 1.7 have been reached in fully non-inductive plasmas (V_{loop} ~ 0) in L-mode and H-mode respectively, both at q_{95} ~ 6,and in presence of good confinement ($H_{98}(y,2)$ ~ 0.8 in L-mode and $H_{98}(y,2)$ ~ 1) using central EC and NB H/CD in the co-Ip direction, which results to f_{BS}<40-50%. Fully non-inductive operation could not be achieved with NBI alone. The plasma loop voltage increases with on-axis NBI while it decreases with off-axis injection in presence of EC waves. Data analyses, interpretative (ASTRA) and predictive (CRONOS suite) modelling confirm this evidence, which is due to an interplay between the plasma density pump-out from ECRH and fuelling from on-axis NBI in the core. Data analyses and interpretative modelling (ASTRA, NUBEAM) also reveals a strong contribution of bulk and FIs to the total plasma pressure and a reduction of the NB heating efficiency due to mainly FI CX losses. The development of plasma scenarios with either internal or external transport barriers has been pursued. ITBs were not formed in either the electron or the ion channel in the plasmas explored to date, despite a significant increase in the toroidal rotation and FI fraction with NBI, which are known to reduce turbulence. The CRONOS suite of codes is used in order to perform transport analyses and as a tool for the preparation of the inputs required for extended gyrokinetic simulations, which will assess whether the plasmas explored in this work are still TEM turbulence dominated, therefore less

prone to be stabilized. The non-inductive sustainment of plasmas with external transport barrier (H-mode) using both EC waves and NBI was successfully attempted. Nonetheless, further scenario development is needed to improve the stability and the performance of these plasmas. Experiments aiming at the steady-state operation of low central magnetic shear H-mode plasmas with $1<q_0<2$ are going to be performed on TCV in the framework of the 2017/18 EUROfusion MST1 campaign.

ACKNOWLEDGEMENTS

This work has been carried out within the framework of the EUROfusion Consortium and has received funding from the Euratom research and training programme 2014-2018 under grant agreement No 633053. The views and opinions expressed herein do not necessarily reflect those of the European Commission.

REFERENCES

[1] KARPUSHOV, A. et al, Upgrade of the TCV tokamak, first phase: Neutral beam heating system, Fusion Eng. Des. **493** (2016) 96-97

[2] VALLAR, M. et al, "Status, scientific results and technical improvements of the NBH on TCV tokamak", 30th edition of the Symposium on Fusion Technology (Proc. Int. Conf. Giardini Naxos, 2018) to be submitted to Fusion Eng. Des.

[3] GNESIN, S. et al, 3rd harmonic electron cyclotron resonant heating absorption enhancement by 2nd harmonic heating at the same frequency in a tokamak, Plasma Phys. Control. Fusion 54 (2012) 035002-17

[4] CODA, S. et al, High-boostrap, noninductively sustained electron internal transport barrier in the Tokamak à Configuration Variable, Phys. of Plasmas **12** (2000) 056124-1

[5] SAUTER, O. et al, Steady-State Fully Noninductive Current Driven by Electron Cyclotron Waves in Magnetically Confined Plasma, Phys. Rev. Lett. **84** 15 (2000) 3322-4

[6] EHRENBERG, J.K., "First Wall Effects on Particle Recycling in Tokamaks", Physical processes of the interaction of fusion plasmas with solids, Academic Press, University of Michigan (1996)

[7] MORET, J. M. et al, Tokamak equilibrium reconstruction code LIUQE and its real time implementation, Fusion Eng. Des. **91** (2015) 1-15

[8] SPITZER, L., Physics of Fully Ionized Gases, Interscience Publishers Inc., New York (1945)

[9] PEREVERZEV, G. V. et al, "ASTRA - Automated System for TRansport Analysis", Max-Planck-Institut Für Plasmaphysik, Garching, 2002

[10] ANDREEV, V. F. et al, Experimental study of density pump-out effect with on-axis electron cyclotron resonance heating at the T-10 tokamak, Plasma Phys. Control. Fusion **58** (20016) 055008-20

[11] MATSUDA, K., Ray Tracing Study of the Electron Cyclotron Current Drive in DIII-D Using 60 GHz, IEEE Trans. Plasma Sci. **17** (1989) 6-11

[12] GARCIA, J. et al, Critical Threshold Behaviour for Steady-State Internal Transport Barriers in Burning Plasmas, Phys. Rev. Lett. 100 (2008)

[13] GOLDSTON, R. J. et al, New techniques for calculating heat and particle source rates due to neutral beam injection in axisymmetric tokamaks, J. Comp. Phys. **43** (1981) 61-78

[14] VALLAR, M. et al, "Nonlinear contribution of neutral beam injection in TCV EC-heated advanced tokamak scenarios", 45th European Physical Society Conference on Plasma Physics (Proc. Int. Conf. Prague, 2018)

[15] GEIGER, B. et al, Fast-ion transport in low density L-mode plasmas at TCV using FIDA spectroscopy and the TRANSP code, Plasma Phys. Control. Fusion **59** (2017) 115002-17

[16] GARCIA, J. et al, Key impact of finite-beta and fast ions in core and edge tokamak regions for the transition to advanced senarios, Nucl. Fusion **55** (2015) 053007-16

[17] ARTAUD, J. F. et al, The CRONOS suite of codes for integrated tokamak modelling, Nucl. Fusion 50 (2010) 043001-26

[18] HONDA, M. et al, Comparison of turbulent transport models of L- and H-mode plasmas, Nucl. Fusion 46 (2006) 580-

[19] LUCE, T. C. et al, Development of advanced inductive scenarios for ITER, Nucl. Fusion **54** (2014) 013015-30